

# Effect of radiation on the crystals of polyethylene and paraffins: 2. Phase separation in $\gamma$ -irradiated paraffins

G. Ungar\*

HH Wills Physics Laboratory, University of Bristol, Tyndall Avenue, Bristol BS8 1TL, UK

Paraffins are observed to respond to  $\gamma$  radiation in a manner which is distinctly different from the behaviour of polyethylene. Namely, the lattice spacings and crystal perfection are virtually unaffected, the destruction of crystallinity becoming manifest through the reduction of the amount of crystalline material and the concurrent increase in the amount of amorphous material ('paraffin-like' behaviour) as opposed to the changes in the crystal lattice and concomitant deterioration of lattice order in polyethylene ('polyethylene-type' behaviour, Part 1). By application of calorimetry, X-ray diffraction and g.p.c. it is seen that the cause underlying the 'paraffin-like' behaviour is a phase segregation between the crosslinked and the still unaffected chains into a liquid-like and an undamaged crystal phase, respectively. There is a thermodynamic equilibrium between these two phases with a limited mutual solubility. The temperature dependence of the latter accounts satisfactorily for the observed melting behaviour ('heterophase' melting) of the irradiated product.

## INTRODUCTION

The effect of ionizing radiation on the crystal lattice in paraffins has received little attention in the past. The only information on this subject so far comes from electron microscope studies. Orth and Fischer<sup>1</sup> investigated the disappearance of electron diffraction from crystals of  $n$ - $C_{28}H_{58}$  during irradiation at room temperature. Contrary to the effects in polyethylene (see Part 1<sup>2</sup>), neither the position nor the width of the reflections changed during the disappearance of crystallinity in this paraffin. This absence of noticeable lattice distortion was attributed to the crystal defects produced by crosslinking being of the quasithermal type. It was assumed that when crosslinked the rigid paraffin chain rotates as a whole into a new lattice position, but the distance between the uncrosslinked molecules in its surroundings remains unaltered. In contrast, polyethylene chains within the crystals *twist* when crosslinked, leading to a large distortion of the lattice.

Here, a different concept is proposed to explain the irradiation behaviour of  $n$ -alkane crystals, and new evidence is included in its support. A number of different long-chain  $n$ -alkanes were  $\gamma$ -irradiated at different temperatures and investigated by X-ray diffraction, thermal analysis and some other methods<sup>†</sup>. Further information

pertinent to the present theme is contained in an extensive microscope study summarized in Part 3<sup>6</sup>. The effect of irradiating the paraffins in different physical states has already been briefly considered in Part 1<sup>2</sup>. Transitions between different crystal modifications can also be induced by irradiation and these will be reported in a separate publication<sup>7</sup>.

## EXPERIMENTAL

A number of  $n$ -paraffins, from  $C_{23}H_{48}$  to  $C_{40}H_{82}$ , were used for  $\gamma$ -irradiation. Most of them were obtained from Sigma Chemicals and were of not less than 99% nominal purity. Prior to irradiation the paraffins were melted under high vacuum to ensure complete exclusion of oxygen. The samples were irradiated in evacuated ampoules in a  $^{60}Co$  source (by courtesy of Professor A. Charlesby and Dr P. J. Fydeler at the Royal Military College of Science at Shrivenham). The dose rate was  $2.7 \text{ Mrad h}^{-1}$ .

Thermal analysis was performed on a Perkin-Elmer DSC-2 calorimeter coupled with a cooling unit. Powder X-ray diffraction patterns were recorded with a Guinier camera and a diffractometer fitted with a heated cell.

## RESULTS

The main characteristics of the X-ray diffraction patterns from all irradiated paraffin crystals are as follows: (a) there is no significant shift in line positions; (b) there is no line broadening; (c) the diffraction intensity decreases with increasing dose and a diffuse halo develops; (d) when the temperature of an irradiated sample is increased, the diffraction line intensity decreases further while the diffuse halo continues to grow. Some of the above features are illustrated in Figure 1. Room temperature diffractograms are shown of an unirradiated and an irradiated sample of  $n$ - $C_{23}H_{48}$ . The maximum observed change in lattice parameters is negligible compared with that for po-

\* Present address: Rudjer Bosković Institute, P.O.B. 1016, 41001 Zagreb, Yugoslavia.

† Paraffin crystals are built up of stacked layers of chain molecules. The chains are either perpendicular or tilted with respect to the layer surface. In the crystals of all paraffins at all irradiation temperatures dealt with in this article the packing mode of methylene groups is the same as in polyethylene crystals, i.e. the subcell is orthorhombic. The complete unit cell is either orthorhombic or monoclinic, depending on chain tilt and layer stacking, but such differences proved to have no significance for the current subject. For simplicity the term 'orthorhombic' will refer hereafter to all paraffins with an orthorhombic subcell. Furthermore, the high temperature modification, sometimes called the 'rotator' phase, will be referred to as the 'hexagonal' phase, although strictly speaking the crystal symmetry is not always fully hexagonal. For reviews on crystallography of  $n$ -alkanes the reader is referred to refs. 3-5.

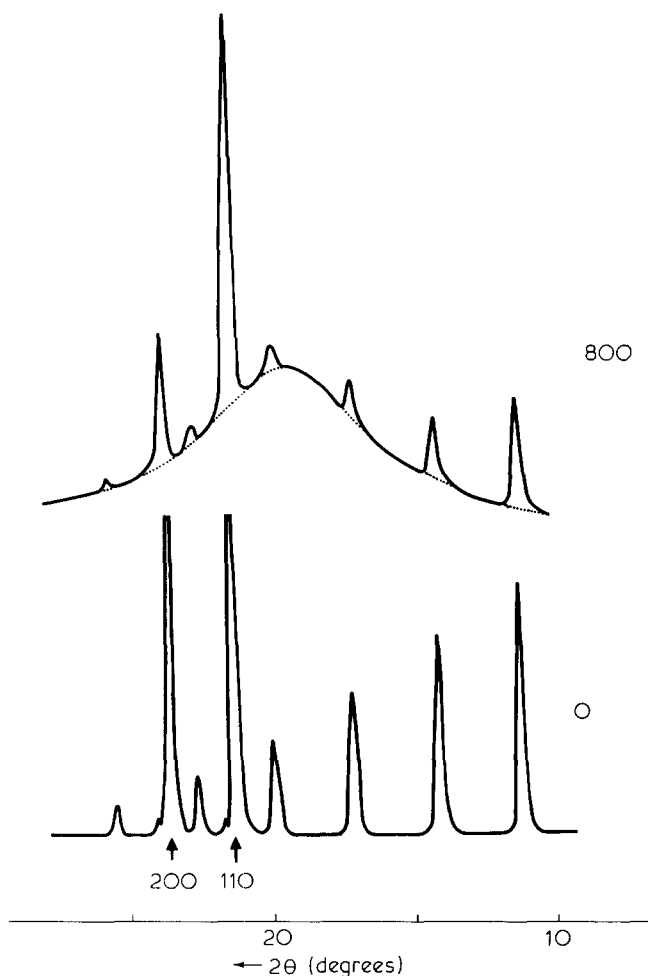


Figure 1 Diffractograms of  $n\text{-C}_{23}\text{H}_{48}$ . Bottom, Unirradiated; top, irradiated at  $33.5^\circ\text{C}$  with 800 Mrad. The strong 110 and 200 lines and the series of 00l reflections are visible. The top diffractogram also shows the amorphous halo

lyethylene (PE). Thus after 1500 Mrad the  $a$ -parameter in  $\text{C}_{40}\text{H}_{82}$  increased by only 0.3%, compared with 5.4% in PE single crystals which received the same dose (see Figure 6).

Furthermore, there is a substantial difference in the thermal behaviour of irradiated paraffins and their polymer counterpart. In PE the temperature of the orthorhombic hexagonal transition,  $T_{o \rightarrow h}$ , decreases with radiation dose more steeply than does the melting temperature,  $T_m$ . The  $o \rightarrow h$  transition endotherm also broadens much more than the melting endotherm. The situation is different in paraffins.  $T_{o \rightarrow h}$  changes only slightly with increasing dose (Figures 2 and 3). Unlike the case of PE, the transition endotherm stays sharp (Figure 4) but the melting peak broadens greatly.  $n\text{-C}_{40}\text{H}_{82}$  does not reveal a solid state transition even when irradiated with high doses.

Another material, which can be regarded as an intermediate between paraffins and PE will now be considered. This is the ozone-degraded, single crystal PE which contains straight alkane chains of about 100 methylene units with a carboxylic group at each end (see Figure 5). On irradiation, the crystal lattice of such degraded polyethylene (DPE) shows a behaviour similar to that of the undegraded polymer, e.g. the  $a$ -parameter greatly increases with dose, etc. (Figure 6 — see also Figure 5 in ref 2).

The thermal behaviour of irradiated DPE is compared with that of the paraffin  $\text{C}_{40}\text{H}_{82}$  in Figure 7. The main reason for using DPE for such a comparison rather than the undegraded PE itself, is that the former, consisting of a crystal phase only is more appropriate for assessment of effects concerning the crystal lattice. As already discussed in Part 1<sup>2</sup> the melting characteristics of irradiated PE are complicated by the fact that a small number of crosslinks can significantly lower the configurational entropy of the melt and thus increase the melting point. This complication is almost negligible in DPE for two reasons: (a) the fold surface is removed and with it the main site for formation of crosslinks<sup>11</sup> — these would affect the entropy of melt but not the crystal lattice; (b) the

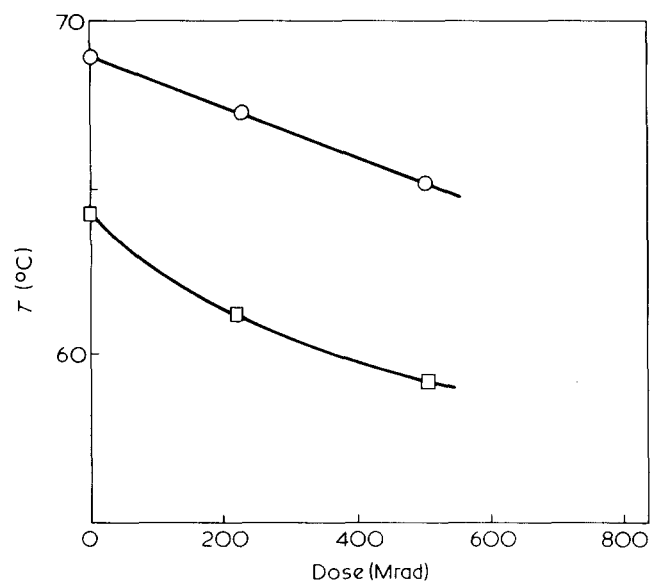


Figure 2 Peak melting ( $\circ$ ) and  $o \rightarrow h$  transition temperature ( $\square$ ) vs. dose for  $n\text{-C}_{32}\text{H}_{66}$  irradiated at  $33.5^\circ\text{C}$

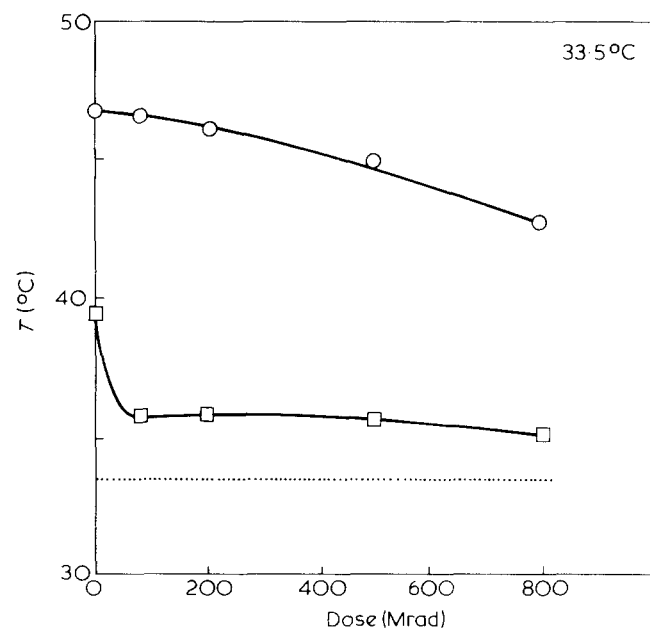


Figure 3 Peak melting ( $\circ$ ) and  $o \rightarrow h$  transition temperature ( $\square$ ) vs. dose for  $n\text{-C}_{23}\text{H}_{48}$ . Broken line marks the irradiation temperature ( $33.5^\circ\text{C}$ )

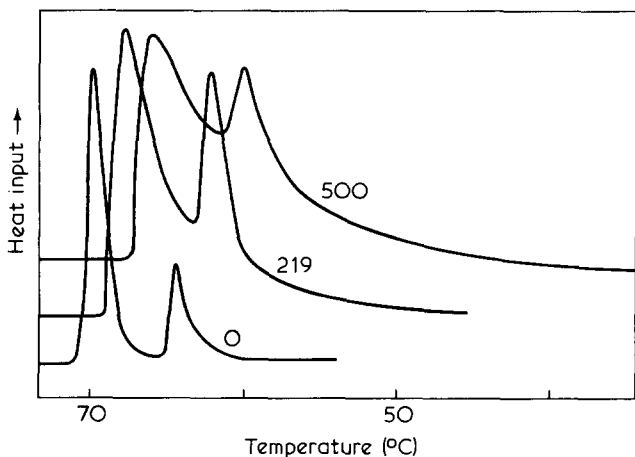


Figure 4 D.s.c. traces of  $n\text{-C}_{32}\text{H}_{66}$  irradiated with 219 and 500 Mrad at  $33.5^\circ\text{C}$  (not normalized). The peaks at the lower and higher temperatures correspond to  $o \rightarrow h$  (transition) and  $h \rightarrow l$  (melting), respectively

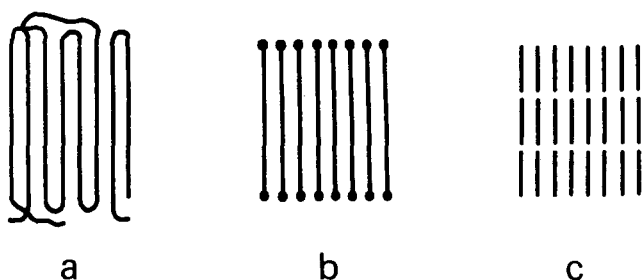


Figure 5 Schematic representation of (a) a single crystal of PE, (b) an ozone-degraded single crystal of PE (DPE) and (c) an n-paraffin crystal. Full circles in (b) represent the  $-\text{COOH}$  groups

molecular weight is drastically reduced. Thus in DPE much fewer molecules are crosslinked for a given dose than in undegraded PE. As an illustration, an infinite gel network (i.e. an average of one effective crosslinked unit per molecule) already forms at 5–10 Mrad in PE<sup>8</sup>, but only at around 1000 Mrad in DPE (room temperature irradiation)<sup>9</sup>. Hence the effect on the entropy of the melt in DPE is small, while the distortion of the crystal lattice remains similar to that in PE.

As seen in Figure 7, both in DPE and in the paraffin,  $T_m$  and the heat of fusion are reduced by irradiation. However, the two materials still behave differently. As stated previously the melting peak of the paraffin broadens greatly, but the maximum  $T_m$  is lowered only slightly. In contrast, the DPE melting peak remains fairly sharp, but its temperature is reduced much more than that of the paraffin (incidentally, the low temperature shoulder in the thermogram of irradiated DPE is believed to represent the onset of the  $o \rightarrow h$  transition).

Finally, one example will be shown of the correlation between calorimetric and gel chromatographic (g.p.c.) data for irradiated paraffins (g.p.c. spectra were obtained by Dr J. Stejny). Whereas only a single peak, corresponding to the parent paraffin, is present in the g.p.c. spectrum of the unirradiated sample ('monomer' peak), additional maxima, corresponding to the crosslinked 'dimer', 'trimer', etc., are observed in the spectra of irradiated paraffins. The 'monomer' weight fraction,  $W_1$ , i.e. the fraction of the still uncrosslinked material, is plotted against radiation dose in Figure 8 for  $n\text{-C}_{40}\text{H}_{82}$  irradiated

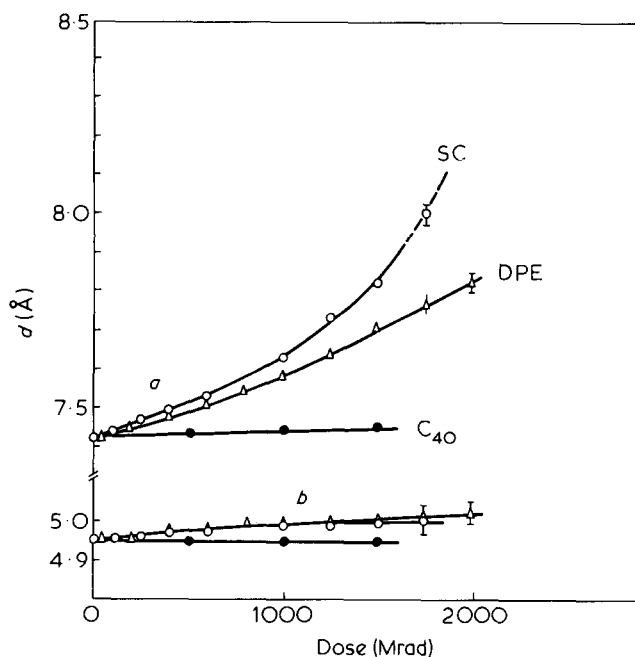


Figure 6 Change in unit cell parameters  $a$  and  $b$  with radiation dose: SC, PE single crystals grown at  $85^\circ\text{C}$  ( $\circ$ ); DPE, degraded PE crystals ( $\Delta$ );  $\text{C}_{40}$ , paraffin  $n\text{-C}_{40}\text{H}_{82}$  ( $\bullet$ ). Irradiation temperature is  $40\text{--}45^\circ\text{C}$  for all these samples

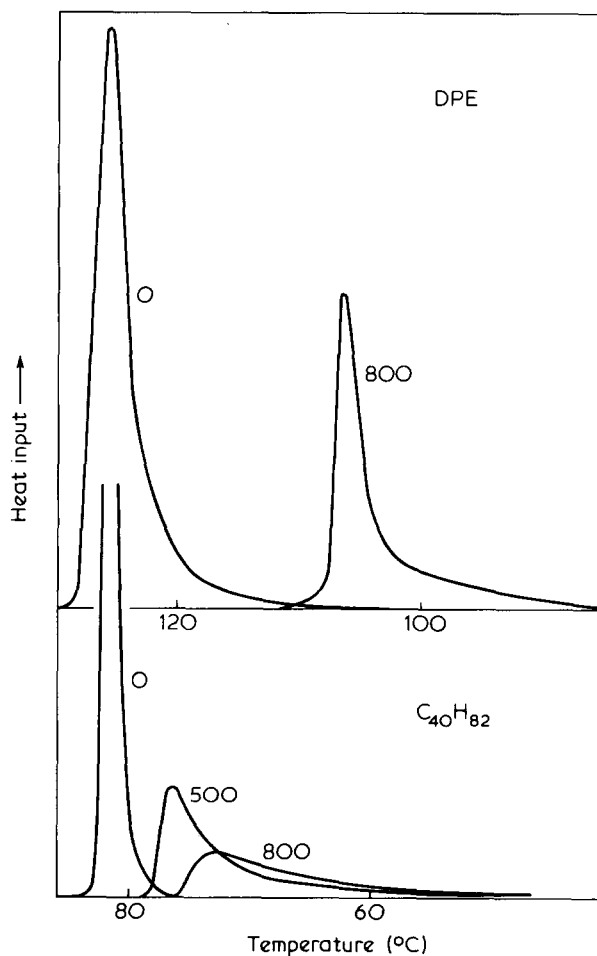


Figure 7 Top, d.s.c. traces of an unirradiated and an irradiated sample of degraded PE (800 Mrad at  $85^\circ\text{C}$ ); Bottom, d.s.c. traces of an unirradiated and two irradiated samples of  $n\text{-C}_{40}\text{H}_{82}$  (500 and 800 Mrad at  $40\text{--}45^\circ\text{C}$ ). Thermograms normalized to the same sample mass. (The numbers 0, 500 and 800 refer to the dose)

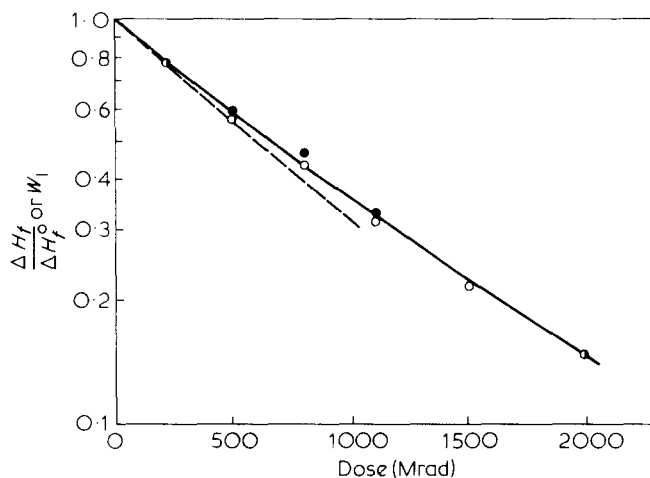


Figure 8 Uncrosslinked weight fraction  $W_1$  as determined by g.p.c. (●) and relative heat of fusion  $\Delta H_f/\Delta H_f^0$  (○) for  $C_{40}H_{82}$  irradiated at  $40^\circ$ – $45^\circ$  C. Initial slope marked with broken line

at  $40$ – $45^\circ$  C (full circles). For samples which received  $\geq 800$  Mrad,  $W_1$  represents the weight ratio of the 'monomer' to the total material, including the insoluble gel. In addition to  $W_1$  the relative heat of fusion is plotted on the same scale in Figure 8 (open circles). The two quantities almost coincide for all doses and both follow a nearly exponential decay. From the slope of  $\log W_1$  vs. dose<sup>10</sup> the initial  $G$  value for crosslinking of  $C_{40}H_{82}$  was determined as 0.95. For comparison, an analogous treatment of the g.p.c. data for DPE irradiated at the same temperature<sup>11</sup> yields a  $G(\text{crosslink})$  value of 0.25.

## DISCUSSION

All the experimental results presented above clearly show a distinct difference in the way irradiation affects the crystal lattice in the thick layer crystals ( $\geq 100$  Å) of PE and DPE and in the thin layer crystals ( $\leq 50$  Å) of *n*-paraffins. However,<sup>12,13</sup> the chemical changes induced in paraffins by radiation are essentially the same as in PE. In both cases the main reactions are crosslinking, formation of *trans*-vinylene unsaturations and some chain scission. The crosslinks are here of primary concern as they are the least compatible with regular chain packing in the orthorhombic crystal lattice (see Introduction to Part 1<sup>2</sup>).

The most rational interpretation of the present results for irradiated paraffins is that crosslinks are not incorporated into the crystal lattice to any significant extent. Therefore, even high radiation doses do not cause a change in unit cell dimensions or a broadening of X-ray lines. At the same time, the development of the diffuse halo in the diffraction patterns of irradiated paraffins indicates the appearance of a separate amorphous phase. The position of the diffuse maximum corresponds to a Bragg spacing of 4.55 Å, which coincides with that for liquid paraffins or the amorphous phase in semicrystalline PE. The naturally emerging picture of an irradiated paraffin is therefore one in which a crystalline phase, mainly free of defects, coexists with a liquid phase which contains most of the crosslinked molecules. The proportion of the liquid phase increases both with increasing radiation dose (increasing fraction of crosslinked molecules) and with increasing temperature (more uncrosslinked, or 'monomer', molecules are dissolved in the liquid phase). At higher radiation doses the liquid will of course turn into an insoluble gel.

The above picture explains the broad melting endotherms of irradiated paraffins. Some 'melt' is already present at room temperature. Furthermore, there is an equilibrium concentration of 'monomer' molecules in the liquid phase and this is higher the higher the temperature. Thus, with any increase in temperature, a certain amount of crystalline 'monomer' is dissolved in the liquid, or, in other words, melted. A process of this kind is sometimes termed 'heterophase melting'<sup>14</sup>. To a first approximation an irradiated paraffin can be regarded as a binary system, the components being the uncrosslinked and the crosslinked portion, respectively (see below).

In those irradiated crystals which show 'polyethylene-like' behaviour, i.e. in PE and DPE, there is no such phase separation. An ever increasing number of crosslinks is built into the crystals. This results in large lattice distortion and in a greatly reduced melting point (Figure 7). Since such crystals remain homogenous, the melting peak remains relatively sharp, i.e. the whole material melts within a narrow temperature interval in which the free energy of the defect crystals coincides with that of the liquid ('homophase melting').

Figures 2 and 3 show that the temperature of the  $o \rightarrow h$  crystal transition in paraffins decreases only slightly with increasing dose. Moreover, the transition endotherm stays sharp. This behaviour is consistent with the above conclusion that the crystalline phase remains almost free of defects. In contrast,  $T_{o \rightarrow h}$  is markedly reduced in the highly-distorted crystals of irradiated PE.

The above concept is graphically represented by Figure 9. Figure 9a shows the schematic binary phase diagram and Figure 9b the corresponding free energies,  $G_o$ ,  $G_h$ , and  $G_l$ , of the orthorhombic, hexagonal and liquid phases as a function of composition for an arbitrarily chosen temperature  $T_{irr}$ . The two chemical components are the uncrosslinked (left) and the crosslinked paraffin (right), and  $X$  is the weight fraction of the latter. The present phase diagram is appropriate for those paraffins which display the hexagonal phase, such as  $C_{23}H_{48}$  or  $C_{32}H_{66}$ . For longer paraffins, such as  $C_{40}H_{82}$ , which retain their orthorhombic subcell up to the melting point, the diagram would be simpler, consisting only of one *solidus* and *liquidus* curve.

Let us assume that irradiation takes place at  $T_{irr}$  and that the system is maintained in equilibrium. A low concentration of crosslinked molecules,  $X_A$ , is tolerated by the orthorhombic lattice, but as this is exceeded a liquid phase forms with a crosslink concentration  $X_C$ .

Assuming now that the crosslink concentration remains constant within the crystals during a d.s.c. heating scan (slight departure from the equilibrium partition) the  $o \rightarrow h$  transition will occur at the temperature  $T_A$ , where  $G_o = G_h$  (if the equilibrium were maintained even during the d.s.c. scan, which is unlikely,  $o \rightarrow h$  transition would occur at the eutectoid temperature  $T_e$ ). Thus, after an initial drop,  $T_{o \rightarrow h}$  would ideally stay constant with further irradiation (see Figures 2 and 3). For any given dose for which  $X_A < X < X_C$  two phases will coexist at  $T_{irr}$ , their weight ratio being determined by the lever rule<sup>15</sup>. The shape of the melting endotherm of such a composite system will be determined to a good approximation by the shape of the *liquidus* curve  $X_l(T)$ : the departure of the calorimeter trace from the baseline would be proportional to  $dX_l/dT$ , causing the characteristic broadening at the low temperature side of the melting endotherms of irradiated paraffins (Figures 4 and 7). The maximum

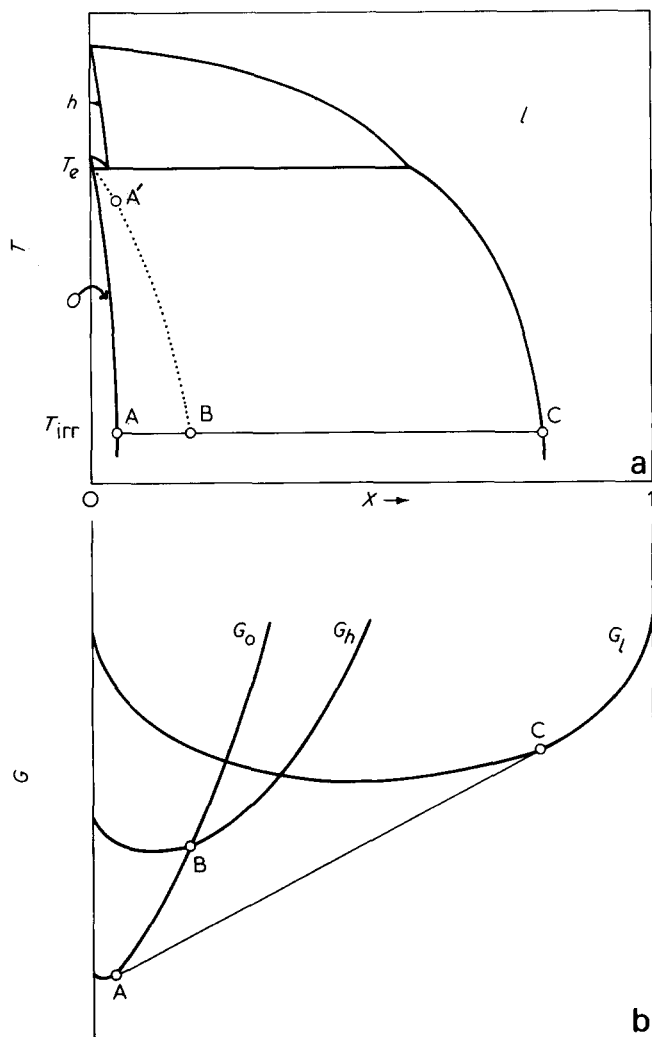


Figure 9 Schematic phase diagram for (a) an irradiated paraffin which undergoes hexagonal transition and (b) the corresponding free energy diagram at the temperature  $T_{irr}$ . Binary system, uncrosslinked (left); crosslinked paraffin (right);  $o$ ,  $h$  and  $l$  denote the orthorhombic, hexagonal and liquid phases, and  $G_o$ ,  $G_h$  and  $G_l$  the respective free energies. Dotted curve joins the points where  $G_o = G_h$ . For further description, see text

melting point is given directly by  $X_A(T)$ . The phase diagram (Figure 9a) also shows that for high radiation doses, at which the maximum melting temperature drops below  $T_A$ , the sample would melt completely without undergoing the hexagonal transition at all. Indeed this situation has been observed experimentally as a merging of the transition and the melting endotherms in those paraffins for which the two endotherms were close together even before irradiation (e.g. paraffin  $C_{22}H_{46}$ , to be described elsewhere<sup>7</sup>).

The close correspondence of  $W_1$ , the uncrosslinked weight fraction and the relative heat of fusion for  $C_{40}H_{82}$  (Figure 8) also supports the concept of phase separation. Moreover, it indicates that the uncrosslinked material is found almost entirely in the crystalline, and the crosslinked material in the non-crystalline phase, at least at room temperature, which is below the temperature at which fusion becomes detectable in the present experiments.

This paper has shown that phase separation is responsible for the 'paraffin-like' irradiation behaviour of n-alkane crystals. The free energy of the two-phase system

proceeds along the line A-C (Figure 9b) with increasing radiation dose. The fact that phase separation does not occur in PE and DPE can either be due to the fact that it is hindered, so that a metastable state is maintained, or else that phase separation is thermodynamically not favoured (e.g.  $G_l$  is much higher than  $G_o$ ). Leaving this question aside, we can nevertheless describe the observed effects in irradiated PE by means of Figure 9b in a qualitative way. This time  $X$  will be taken simply as a parameter proportional to the crosslink density. With increasing  $X$  the free energy of the crystals proceeds along curve  $G_o$  up to the point B at which the  $o \rightarrow h$  transition occurs. At room temperature this happens around 2200 Mrad for PE single crystals and around 2800 Mrad for quenched bulk PE (Figure 5 of Part 1<sup>2</sup>). With a further increase in  $X$ , curve  $G_h$  is followed up to its intersection with  $G_l$ , when crystallinity is finally destroyed. Similarly, if a PE sample with  $X < X_B$  is heated the  $o \rightarrow h$  transition can occur if, for the corresponding crosslink density,  $G_h$  falls below the free energies of the other two phases.

Finally the way in which phase separation is brought about in irradiated paraffins will be briefly considered. The question arises as to whether the crosslinks form within the crystalline phase and subsequently are excluded from it, or whether crosslinking is confined to the liquid phase which already appears at low irradiation doses. The latter mechanism would require the radiation-induced active sites, which are formed at random throughout the material, to migrate to the liquid phase, or else the crosslinking efficiency would increase markedly with dose as the liquid fraction increases. Figure 8 shows that, if anything, the crosslinking efficiency decreases slightly with dose. In Part 3 of this series<sup>6</sup> it will be shown that the active sites can indeed migrate rapidly through irradiated crystalline paraffins. Electron microscopically identifiable non-crystalline regions form within the crystals. The high rate of formation of these regions is incompatible with diffusion of whole crosslinked molecules and hence it is concluded that the large majority of crosslinks actually form within the liquid 'droplets'. However, whether those crosslinks which still happen to form within the crystalline phase can also subsequently segregate from it is uncertain at present. There is certain evidence that the latter can occur, given enough time<sup>7</sup>. It is believed that there is sufficient driving force for exclusion of crosslinks from the crystal lattice. This is judged from the high elastic strain energy of a crosslink within the orthorhombic crystal (35 kcal mol<sup>-1</sup>) as recently calculated by Guui<sup>16</sup>.

## ACKNOWLEDGEMENTS

My thanks are due to Dr J. Stejny for his active contribution to the g.p.c. analysis and for his constructive advice throughout this work, and to Professor A. Keller for suggestion of the subject matter, general interest and advice on the manuscript. I am indebted to Professor A. Charlesby and Dr P. Fydeler, Royal Military College, Shrivenham for the irradiation of samples and wish to thank the Science Research Council for financial support.

## REFERENCES

- 1 Orth, H. and Fischer, E. W. *Makromol. Chem.* 1965, **88**, 188
- 2 Ungar, G. and Keller, A. *Polymer* 1980, **21**, 000

- 3 Kitaigorodskii, A. I., 'Organic Chemical Crystallography', Consultants Bureau, New York, 1961, Ch 4
- 4 Broadhurst, H. G. *J. Res. Nat. Bur. Stand.* 1962, **66A**, 241
- 5 Piesczek, W., Strobl, G. R. and Malzahn, K. *Acta Crystallogr. (B)* 1974, **30**, 1278
- 6 Ungar, G., Grubb, D. T. and Keller, A. *Polymer* 1980, **21**, 000
- 7 Ungar, G., in preparation
- 8 Patel, G. N. and Keller, A. *J. Polym. Sci. (Polym. Phys. Edn)* 1975, **13**, 339
- 9 Stejny, J. personal communication
- 10 Flory, P. J. *J. Am. Chem. Soc.* 1941, **63**, 3096
- 11 Patel, G. N. and Keller, A. *J. Polym. Sci. (Polym. Phys. Edn)* 1975, **13**, 303
- 12 Topchiev, A. V. 'Radiolysis of Hydrocarbons' Elsevier, Amsterdam, 1964
- 13 Falconer, W. and Salovey, R. *J. Chem. Phys.* 1966, **44**, 3151
- 14 Ubbelohde, A. R. 'Melting and Crystal Structure', Clarendon Press, Oxford, 1965
- 15 Rhines, F. N. 'Phase Diagrams in Metallurgy' McGraw-Hill, New York, 1956
- 16 Guiu, F. and Shadrake, L. G. *Proc. Roy. Soc. (London)* 1975 **A346**, 305; also F. Guiu, Personal communication